

# A malignant hyperthermia–inducing mutation in RYR1 (R163C): consequent alterations in the functional properties of DHPR channels

Roger A. Bannister,<sup>1</sup> Eric Estève,<sup>2,3</sup> José M. Eltit,<sup>2,4</sup> Isaac N. Pessah,<sup>5</sup> Paul D. Allen,<sup>2</sup> José R. López,<sup>2</sup> and Kurt G. Beam<sup>1</sup>

<sup>1</sup>Department of Physiology and Biophysics, School of Medicine, University of Colorado-Anschutz Medical Campus, Aurora, CO 80045

<sup>2</sup>Department of Anesthesiology Perioperative and Pain Medicine, Brigham and Women's Hospital, Boston, MA 02115

<sup>3</sup>Université Victor Segalen Bordeaux 2, Institut National de la Santé et de la Recherche Médicale U885, Laboratoire de Physiologie Cellulaire Respiratoire, 33076 Bordeaux, France

<sup>4</sup>Programa de Biología Molecular y Celular, Instituto de Ciencias Biomedicas Facultad de Medicina, Universidad de Chile, Casilla 70005, Santiago, Chile

<sup>5</sup>Department of Molecular Biosciences, School of Veterinary Medicine, University of California, Davis, Davis, CA 95616

Bidirectional communication between the 1,4-dihydropyridine receptor (DHPR) in the plasma membrane and the type 1 ryanodine receptor (RYR1) in the sarcoplasmic reticulum (SR) is responsible for both skeletal-type excitation–contraction coupling (voltage-gated  $\text{Ca}^{2+}$  release from the SR) and increased amplitude of L-type  $\text{Ca}^{2+}$  current via the DHPR. Because the DHPR and RYR1 are functionally coupled, mutations in RYR1 that are linked to malignant hyperthermia (MH) may affect DHPR activity. For this reason, we investigated whether cultured myotubes originating from mice carrying an MH-linked mutation in RYR1 (R163C) had altered voltage-gated  $\text{Ca}^{2+}$  release from the SR, membrane-bound charge movement, and/or L-type  $\text{Ca}^{2+}$  current. In myotubes homozygous (Hom) for the R163C mutation, voltage-gated  $\text{Ca}^{2+}$  release from the SR was substantially reduced and shifted ( $\sim 10$  mV) to more hyperpolarizing potentials compared with wild-type (WT) myotubes. Intramembrane charge movements of both Hom and heterozygous (Het) myotubes displayed hyperpolarizing shifts similar to that observed in voltage-gated SR  $\text{Ca}^{2+}$  release. The current–voltage relationships for L-type currents in both Hom and Het myotubes were also shifted to more hyperpolarizing potentials ( $\sim 7$  and  $5$  mV, respectively). Compared with WT myotubes, Het and Hom myotubes both displayed a greater sensitivity to the L-type channel agonist  $\pm$ Bay K 8644 ( $10 \mu\text{M}$ ). In general, L-type currents in WT, Het, and Hom myotubes inactivated modestly after 30-s prepulses to  $-50$ ,  $-10$ ,  $0$ ,  $10$ ,  $20$ , and  $30$  mV. However, L-type currents in Hom myotubes displayed a hyperpolarizing shift in inactivation relative to L-type currents in either WT or Het myotubes. Our present results indicate that mutations in RYR1 can alter DHPR activity and raise the possibility that this altered DHPR function may contribute to MH episodes.

## INTRODUCTION

In skeletal muscle, the L-type  $\text{Ca}^{2+}$  channel (or 1,4-dihydropyridine receptor [DHPR]) serves as the voltage sensor (Schneider and Chandler, 1973; Ríos and Brum, 1987; Tanabe et al., 1988) for excitation–contraction coupling (ECC) by triggering the opening of the type 1 ryanodine-sensitive SR  $\text{Ca}^{2+}$  release channel (RYR1) in the SR. This “orthograde” signal appears to be mediated by conformational coupling between the DHPR and RYR1 because ECC is rapid, persists in the absence of extracellular  $\text{Ca}^{2+}$  (Armstrong et al., 1972; Tanabe et al., 1990), and can be restored in dysgenic (DHPR  $\alpha_{1S}$  subunit null) myotubes by expression of an  $\alpha_{1S}$  subunit (SkEIIIK) with a very low  $\text{Ca}^{2+}$  permeability (Dirksen and Beam, 1999; Bannister et al., 2009b). In addition to the orthograde ECC signal from the DHPR to RYR1,

there is also a retrograde signal whereby RYR1 increases the magnitude of the L-type  $\text{Ca}^{2+}$  current generated by the DHPR, most likely as a consequence of increased channel  $P_o$  (Nakai et al., 1996). This retrograde effect of RYR1 is independent of SR  $\text{Ca}^{2+}$  release (Grabner et al., 1999; Hurne et al., 2005) and affects not only the magnitude of the current, but also activation kinetics (Avila and Dirksen, 2000; Ahern et al., 2003; Sheridan et al., 2006).

The existence of physical links between DHPRs and RYR1 is strongly supported by freeze-fracture analyses that reveal that intramembranous particles, which are likely to be DHPRs in the plasma membrane at sites of junction with the SR, are arranged into “tetrads” with a spacing that places them in register with the four subunits of every other RYR1 (Block et al., 1988;

Correspondence to Kurt G. Beam: kurt.beam@ucdenver.edu

Abbreviations used in this paper: DHPR, 1,4-dihydropyridine receptor; ECC, excitation–contraction coupling; Het, heterozygous; Hom, homozygous; MH, malignant hyperthermia; MHS, MH-susceptible; WT, wild-type.

© 2010 Bannister et al. This article is distributed under the terms of an Attribution–Noncommercial–Share Alike–No Mirror Sites license for the first six months after the publication date (see <http://www.rupress.org/terms>). After six months it is available under a Creative Commons License (Attribution–Noncommercial–Share Alike 3.0 Unported license, as described at <http://creativecommons.org/licenses/by-nc-sa/3.0/>).

Takekura et al., 1994, 2004; Protasi et al., 2002; Sheridan et al., 2006). Moreover, a conformational change of RYR1 that is induced by exposure to high ryanodine causes a 2-nm decrease in distance between adjacent tetradic particles, further supporting the hypothesis that DHPRs are docked to RYR1 (Paolini et al., 2004). Treatment with ryanodine similar to that causing rearrangement of tetradic particles also alters DHPR gating (Bannister and Beam, 2009). Thus, the retrograde signal appears to depend upon the conformation of RYR1.

Given the evidence that RYR1 has retrograde effects on DHPR function, and that this retrograde signal is affected by RYR1 conformation as described above, the question naturally arises of whether malignant hyperthermia (MH)-causing mutations in RYR1 affect DHPR function. Recently, alterations in the function of the DHPR as ECC voltage sensor and as an L-type  $\text{Ca}^{2+}$  channel have been reported in muscle cells harvested from mice carrying the MH-linked Y522S mutation of RYR1 (Chelu et al., 2006; Durham et al., 2008; Andronache et al., 2009). In the present study, we have used whole cell patch clamping to assess directly the effects of another MH-linked mutation in RYR1 (R163C) on currents generated by DHPR. We found that the R163C mutation alters multiple aspects of the function of the DHPR as both ECC voltage sensor and as L-type  $\text{Ca}^{2+}$  channel, raising the possibility that altered DHPR activity may contribute to the pathophysiology associated with at least some of the MH-causing mutations of RYR1.

## MATERIALS AND METHODS

### Myotube culture

The University of Colorado-Anschutz Medical Campus and Harvard Medical School Institutional Animal Care and Use Committees approved all procedures involving mice. Myoblast cell lines were generated from the limb muscles of neonatal heterozygous (Het) and homozygous (Hom) F2 MHR163C C57Bl6/129svJ mice and their wild-type (WT) littermates (Rando and Blau, 1994; Yang et al., 2006). Myoblasts were differentiated into myotubes by withdrawal of growth factors, as described previously (Yang et al., 2003), and used in electrophysiological experiments 5–7 d later.

### Measurement of intracellular $\text{Ca}^{2+}$ transients

All experiments were performed at room temperature ( $\sim 25^\circ\text{C}$ ). Changes in intracellular  $\text{Ca}^{2+}$  were recorded with Fluo-3 (Invitrogen) in the whole cell patch clamp configuration (see below). The salt form of the dye was added to the standard internal solution (see below) for a final concentration of 200  $\mu\text{M}$ . After entry into the whole cell configuration, a waiting period of  $>5$  min was used to allow the dye to diffuse into the cell interior. A 100-W mercury illuminator and a set of fluorescein filters were used to excite the dye present in a small rectangular region of the voltage-clamped myotube. A computer-driven shutter was used to block illumination in the intervals between 50-ms test pulses. Fluorescence emission was measured by means of a fluorometer apparatus (Biomedical Instrumentation Group, University of Pennsylvania, Philadelphia, PA). The average background fluorescence was quantified before bath immersion of the patch pipette. Fluorescence data are expressed as  $\Delta F/F$ , where  $\Delta F$  represents the change in peak fluorescence from

baseline during the test pulse, and  $F$  is the fluorescence immediately before the test pulse minus the average background (non-Fluo-3) fluorescence. The peak value of the fluorescence change ( $\Delta F/F$ ) for each test potential ( $V$ ) was fitted according to:

$$\Delta F/F = [\Delta F/F]_{\max} / \left[ 1 + \exp\left\{-\frac{(V - V_F)}{k_F}\right\}\right], \quad (1)$$

where  $[\Delta F/F]_{\max}$  is the maximal fluorescence change,  $V_F$  is the potential causing half the maximal change in fluorescence, and  $k_F$  is a slope parameter.

### Electrophysiology

Pipettes were fabricated from borosilicate glass and had resistances of  $\sim 1.5$  M $\Omega$  when filled with internal solution, which consisted of (in mM): 140 Cs-aspartate, 10 Cs<sub>2</sub>-EGTA, 5 MgCl<sub>2</sub>, and 10 HEPES, pH 7.4 with CsOH. The external solution contained (in mM): 145 tetraethylammonium-Cl, 10 CaCl<sub>2</sub>, 0.003 tetrodotoxin, and 10 HEPES, pH 7.4 with tetraethylammonium-OH. In some experiments, myotubes were exposed to racemic Bay K 8644 (provided by A. Scriabine, Miles Laboratories Inc., New Haven, CT) in the bath solution. Racemic Bay K 8644 was stored as a 20-mM stock in 50% EtOH and was diluted in the external recording solution just before experiments.

For measurement of charge movements, ionic currents were blocked by the addition of 0.5 mM CdCl<sub>2</sub> plus 0.1 mM LaCl<sub>3</sub> to the extracellular recording solution. All charge movements were corrected for linear cell capacitance and leakage currents using a  $-P/8$  subtraction protocol (Bannister et al., 2008a,b, 2009a). Filtering was at 2 kHz (eight-pole Bessel filter; Frequency Devices, Inc.), and digitization was at 20 kHz. Voltage clamp command pulses were exponentially rounded with a time constant of 50–500  $\mu\text{s}$ , and a 1-s prepulse to  $-20$  mV, followed by a 50-ms repolarization to  $-50$  mV, was administered before the test pulse (prepulse protocol; see Adams et al., 1990) to reduce the contribution of gating currents from voltage-gated Na<sup>+</sup> channels and low voltage-activated  $\text{Ca}^{2+}$  channels. The integral of the ON transient ( $Q_{\text{on}}$ ) for each test potential ( $V$ ) was fitted according to:

$$Q_{\text{on}} = Q_{\max} / \left\{ 1 + \exp\left[-\frac{(V - V_Q)}{k_Q}\right] \right\}, \quad (2)$$

where  $Q_{\max}$  is the maximal  $Q_{\text{on}}$ ,  $V_Q$  is the potential causing movement of half the maximal charge, and  $k_Q$  is a slope parameter.

For generation of I-V relationships, linear capacitive and leakage currents were determined by averaging the currents elicited by 11 30-mV hyperpolarizing pulses from the holding potential of  $-80$  mV. Test currents were corrected for linear components of leak and capacitive current by digital scaling and subtraction of this average control current. In all other experiments,  $-P/4$  subtraction was used. Electronic compensation was used to reduce the effective series resistance (usually to  $<1$  M $\Omega$ ) and the time constant for charging the linear cell capacitance (usually to  $<0.5$  ms). L-type currents were filtered at 2 kHz and digitized at 5–10 kHz. In most cases, the prepulse protocol (see above) was used to inactivate low voltage-activated  $\text{Ca}^{2+}$  channels. Cell capacitance was determined by integration of a transient evoked by stepping from  $-80$  to  $-70$  mV using Clampex 8.0 (MDS Analytical Technologies) and was used to normalize current amplitudes (pA/pF). I-V curves were fitted using the following equation:

$$I = G_{\max} * (V - V_{\text{rev}}) / \left\{ 1 + \exp\left[-\frac{(V - V_{1/2})}{k_G}\right] \right\}, \quad (3)$$

where  $I$  is the peak current for the test potential  $V$ ,  $V_{\text{rev}}$  is the reversal potential,  $G_{\max}$  is the maximum  $\text{Ca}^{2+}$  channel conductance,  $V_{1/2}$  is the half-maximal activation potential, and  $k_G$  is the slope

factor. The activation phase of L-type currents was fitted using the following exponential function:

$$I(t) = A_{\text{fast}}[\exp(-t/\tau_{\text{fast}})] + A_{\text{slow}}[\exp(-t/\tau_{\text{slow}})] + C, \quad (4)$$

where  $I(t)$  is the current at time  $t$  after the depolarization,  $A_{\text{fast}}$  and  $A_{\text{slow}}$  are the steady-state current amplitudes of each component with their respective time constants of activation ( $\tau_{\text{fast}}$  and  $\tau_{\text{slow}}$ ), and  $C$  represents the steady-state current (see Avila and Dirksen, 2000).

In steady-state inactivation experiments, cells were held at prepulse potentials ( $-50$ ,  $-10$ ,  $0$ ,  $10$ ,  $20$ , and  $30$  mV) for 30 s before a 200-ms test depolarization to  $+30$  mV. To minimize the cumulative effects of holding at less negative potentials, an interval of  $>1$  min at the steady holding potential ( $-80$  mV) was maintained between each test pulse and the subsequent prepulse (see Beam and Knudson, 1988). Steady-state inactivation curves were fit by the Boltzmann equation:

$$I/I_0 = 1 - 1 / (1 + \exp[-(V - V_{1/2\text{inact}})/k]), \quad (5)$$

where  $I$  is the current amplitude for a test depolarization to  $+30$  mV immediately after a 30-s prepulse  $V$ ,  $I_0$  is the current amplitude of a reference pulse from  $-80$  to  $+30$  mV evoked just before each prepulse,  $V_{1/2\text{inact}}$  is the half-maximal inactivation potential, and  $k$  is the slope factor.

#### Analysis

Figures were made using the software program SigmaPlot (version 11.0; SPSS Inc.). All data are presented as mean  $\pm$  SEM. Statistical comparisons were by ANOVA or unpaired, two-tailed  $t$  test (as appropriate), with  $P < 0.05$  considered significant.

## RESULTS

SR  $\text{Ca}^{2+}$  release is shifted to more hyperpolarized potentials in R163C myotubes

Because the R163C mutation was shown to cause  $\text{Ca}^{2+}$  to be released from the SR in response to smaller elevations of extracellular  $\text{K}^+$  applied to intact myotubes (Yang et al., 2006; Estève et al., 2010), we sought to determine whether a corresponding effect occurred in myotubes subjected to whole cell patch clamp. To assess directly the effects of the R163C mutation on voltage-triggered  $\text{Ca}^{2+}$  release, without complications from RYR1 tetramers having variable WT/mutant monomer stoichiometry, we initially compared  $\text{Ca}^{2+}$  transients of myotubes Hom for the R163C mutation with those of WT myotubes. As shown in Fig. 1 A, WT myotubes produced robust  $\text{Ca}^{2+}$  transients with an average  $[\Delta\text{F}/\text{F}]_{\text{max}}$  of  $0.76 \pm 0.15$  ( $n = 11$ ). In contrast, R163C Hom myotubes yielded  $\text{Ca}^{2+}$  transients that were considerably smaller in magnitude ( $[\Delta\text{F}/\text{F}]_{\text{max}} = 0.29 \pm 0.09$ ;  $n = 6$ ;  $P < 0.05$ ; Fig. 1 B). Such a reduction in the magnitude of SR  $\text{Ca}^{2+}$  release was most likely related to reductions in DHPR expression (see below). The reduction in  $[\Delta\text{F}/\text{F}]_{\text{max}}$  observed for Hom myotubes was accompanied by a substantial ( $\sim 10$  mV;  $P < 0.05$ ) hyperpolarizing shift in the voltage dependence of  $\text{Ca}^{2+}$  release

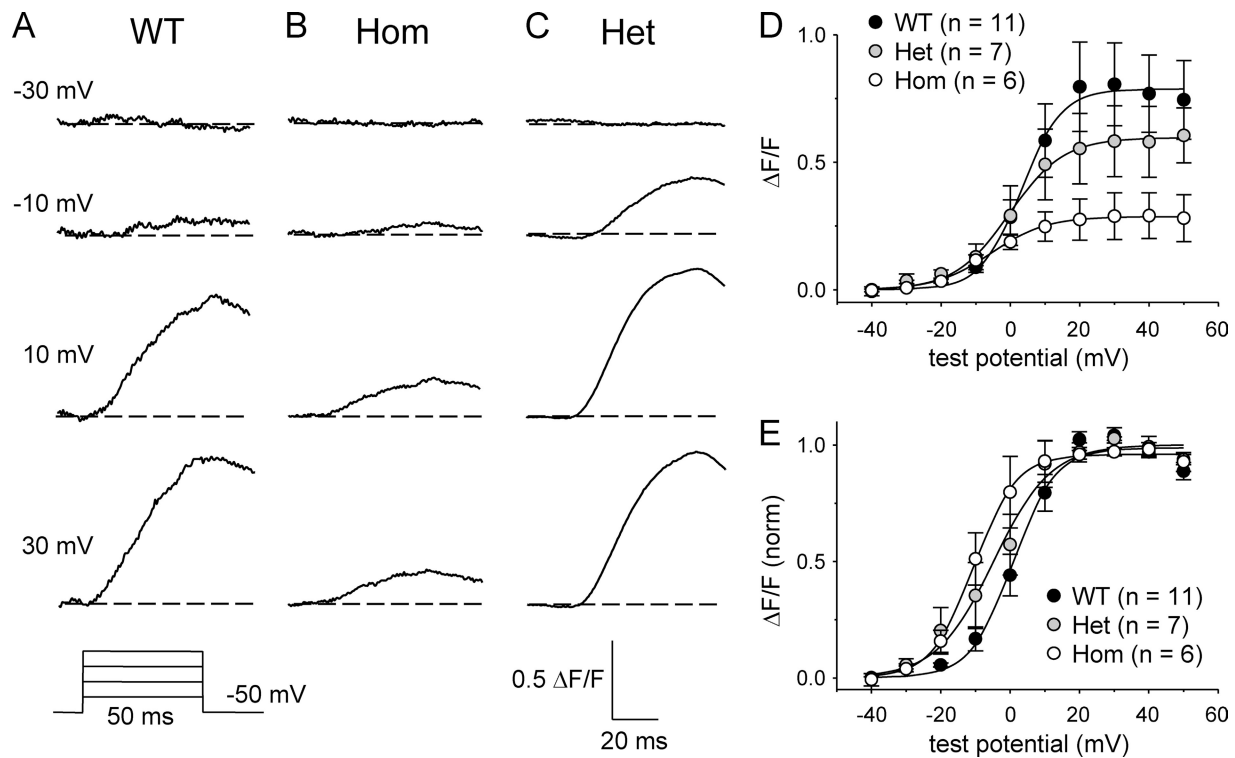


**Figure 1.** SR  $\text{Ca}^{2+}$  release is shifted to more hyperpolarized potentials in R163C MHS myotubes. Representative myoplasmic  $\text{Ca}^{2+}$  transients elicited by 50-ms depolarizations from  $-50$  mV to test potentials of  $-30$ ,  $-10$ ,  $10$ , and  $30$  mV are shown for WT (A), Hom (B), and Het (C) myotubes. Raw  $\Delta\text{F}/\text{F}$ -V relationships are shown in D. The average  $\Delta\text{F}/\text{F}$ -V relationships, obtained after normalizing to the  $[\Delta\text{F}/\text{F}]_{\text{max}}$  in each individual experiment, are shown in E, with the smooth curves plotted according to Eq. 1 and best-fit parameters presented in Table I. Error bars represent  $\pm$  SEM.

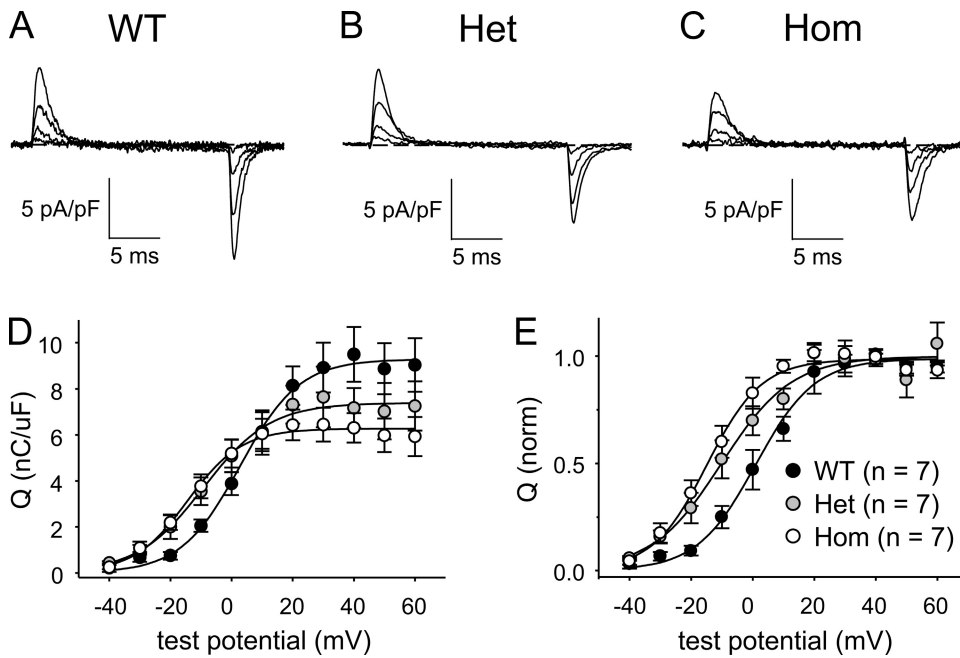


**Figure 2.** Charge movements are shifted to more hyperpolarized potentials in R163C Het and Hom myotubes. Representative charge movements elicited by 20-ms depolarizations from  $-50$  mV to test potentials of  $-30$ ,  $-10$ ,  $10$ , and  $30$  mV are shown for WT (A), Het (B), and Hom (C) myotubes. Raw  $Q$ - $V$  relationships are shown in D. The average  $Q$ - $V$  relationships, obtained after normalizing to the  $Q_{\max}$  in each individual experiment, are shown in E, with the smooth curves plotted according to Eq. 2 and best-fit parameters presented in Table II.

(Fig. 1 D and Table I). This shift was more evident when the respective  $\Delta F/F$ - $V$  curves were normalized to the peak  $\Delta F/F$  in each experiment (Fig. 4 E). Consistent with previous studies in intact myotubes (Yang et al., 2006; Cherednichenko et al., 2008), the voltage dependence of myoplasmic  $Ca^{2+}$  release for Het myotubes ( $V_{1/2F} = -3.8 \pm 4.3$  mV;  $n = 7$ ) was intermediate between those of WT and Hom myotubes (Fig. 1, C-E, and Table I).

#### The R163C mutation reduces DHPR expression and alters the voltage dependence of charge movement

We recorded membrane-bound charge movements to investigate the possibility that the hyperpolarizing shifts in the  $\Delta F/F$ - $V$  relationships for R163C MHS-susceptible (MHS) myotubes were related to similar hyperpolarizing shifts in charge movement. Substantial charge movements were present in the myotubes of all three genotypes (Fig. 2, A-C). The magnitude of the charge movements was reduced in both Het and Hom myotubes ( $Q_{\max} = 7.4 \pm 1.0$  nC/ $\mu$ F;  $n = 7$ , and  $6.4 \pm 0.7$  nC/ $\mu$ F;  $n = 7$ , respectively) compared with WT myotubes ( $9.9 \pm 1.1$  nC/ $\mu$ F;  $n = 7$ ), although this reduction was significant only for Hom ( $P < 0.05$  by  $t$  test; Table II). The reductions in maximal charge movement indicate decreases in the number of functional DHPRs in the plasma membranes of both R163C Het and Hom myotubes. The  $Q$ - $V$  relationships were shifted  $\sim 10$  mV in the hyperpolarizing direction for both Het and Hom myotubes ( $V_{1/2} = -9.9 \pm 2.9$  and  $-13.7 \pm 2.3$  mV, respectively) relative to WT myotubes ( $1.8 \pm 2.9$  mV;  $P < 0.005$ , ANOVA; Fig. 2 D and Table II).

The R163C mutation causes a small hyperpolarizing shift in the activation of L-type current

We next examined whether the R163C mutation also caused changes in L-type currents generated by the DHPR. Representative L-type currents recorded from WT, Het, and Hom myotubes are illustrated in Fig. 3 A. The L-type currents in Het and Hom myotubes differed in two small respects from those in WT myotubes. First, as shown in Fig. 3 B, peak current amplitudes in Het ( $-9.9 \pm 0.7$  pA/pF at  $+30$  mV;  $n = 22$ ) and Hom ( $-9.4 \pm 0.6$  pA/pF at  $+30$  mV;  $n = 28$ ) myotubes were reduced ( $P < 0.05$ , ANOVA) compared with WT myotubes ( $-12.6 \pm 1.1$  pA/pF at  $+40$  mV;  $n = 25$ ). These reductions in maximal current density for Het and Hom myotubes were proportional to the respective reductions in  $Q_{\max}$  (see Fig. 2 D), as indicated by the nearly identical  $G_{\max}/Q_{\max}$  ratios (Table II). Second, comparison of the

TABLE I  
 $\Delta F/F$ - $V$  fit parameters

Genotype	$\Delta F/F$ - $V$		
	$[\Delta F/F]_{\max}$	$V_F$ mV	$k_F$ mV
WT	$0.76 \pm 0.15$ (11)	$1.5 \pm 2.3$	$4.4 \pm 0.4$
Het	$0.56 \pm 0.13$ (7)	$-3.8 \pm 4.3$	$4.8 \pm 0.6$
Hom	$0.29 \pm 0.09^a$ (6)	$-7.7 \pm 3.5^a$	$6.2 \pm 0.9^a$

Average values of parameters obtained by fits of Eq. 1 to  $\Delta F/F$ - $V$  data (see Materials and methods). Data are given as mean  $\pm$  SEM, with the numbers in parentheses indicating the number of myotubes tested.

<sup>a</sup>Significant differences from WT myotubes ( $P < 0.05$ ,  $t$  test).

TABLE II  
Charge movement and conductance fit parameters

Genotype/treatment	Q-V			I-V			G/Q
	Q <sub>max</sub> nC/μF	V <sub>Q</sub> mV	k <sub>Q</sub> mV	G <sub>max</sub> nS/nF	V <sub>1/2</sub> mV	k <sub>G</sub> mV	G <sub>max</sub> /Q <sub>max</sub> nS/pC
WT	9.9 ± 1.1 (7)	1.8 ± 2.9	8.9 ± 0.6	300 ± 18 (25)	24.8 ± 1.2	6.0 ± 0.2	30
WT + Bay K 8644		ND		256 ± 16 (9)	15.4 ± 1.7 <sup>a</sup>	5.6 ± 0.4	ND
Het	7.4 ± 1.0 (7)	-9.9 ± 2.9 <sup>b</sup>	10.2 ± 1.3	229 ± 14 <sup>c</sup> (22)	19.7 ± 1.2 <sup>c</sup>	5.9 ± 0.2	31
Het + Bay K 8644		ND		254 ± 28 (6)	11.7 ± 1.4 <sup>a</sup>	6.0 ± 0.2	ND
Hom	6.4 ± 0.7 <sup>b</sup> (7)	-13.7 ± 2.3 <sup>a</sup>	8.8 ± 1.1	208 ± 10 <sup>a</sup> (28)	17.9 ± 1.1 <sup>a</sup>	6.0 ± 0.3	32
Hom + Bay K 8644		ND		254 ± 28 (9)	11.2 ± 1.3 <sup>a</sup>	6.4 ± 0.3	ND

Average values of parameters obtained by fits of Eqs. 2 and 3 to Q-V and I-V data, respectively (see Materials and methods). Where indicated, myotubes were exposed to 10 μM ±Bay K 8644 for >10 min before experiments. Data are given as mean ± SEM, with the numbers in parentheses indicating the number of myotubes tested. ND, not determined.

<sup>a</sup>Significant differences compared to L-type currents or charge movements recorded from untreated WT myotubes; P < 0.001, *t* test.

<sup>b</sup>P < 0.05, *t* test.

<sup>c</sup>P < 0.005, *t* test.

peak I-V relationships of each genotype revealed small hyperpolarizing shifts in activation of both Het and Hom L-type currents (V<sub>1/2</sub> = 19.7 ± 1.2 and 17.9 ± 1.1 mV, respectively) relative to WT myotubes (V<sub>1/2</sub> = 24.8 ± 1.2 mV; P < 0.001, ANOVA; Table II). These shifts were more clearly evident when the I-V data were normalized to the maximum current in each individual experiment (Fig. 3 C).

L-type current activation kinetics appeared slightly faster in Het and Hom myotubes than in WT myotubes (when compared at +40 mV; Table III), owing to a reduction in the contribution of the slow component of activation to the total current amplitude (P < 0.05, ANOVA). However, these subtle changes in activation may have been related to the shifted I-V relationships

and/or reduced current densities observed in the R163C MHS myotubes.

#### L-type currents of R163C myotubes are more sensitive to ±Bay K 8644

Williams et al. (1991) showed that Bay K 8644 lowers the threshold for halothane-induced contractures in MHS swine muscle fibers. Because the DHPR is the molecular target for Bay K 8644, we tested directly how this agonist affected L-type currents in R163C Het and Hom myotubes. As shown previously (Adams and Beam, 1989), L-type currents of WT myotubes were only weakly potentiated by ±Bay K 8644 (Fig. 4 A). In contrast, the potentiation of L-type currents by ±Bay K 8644 (10 μM) was appreciable in Het myotubes (Fig. 4 B),

TABLE III  
Activation fit parameters

Genotype	I <sub>slow</sub>			I <sub>fast</sub>		
	τ <sub>slow</sub> ms	A <sub>slow</sub> pA/pF	Fraction (%)	τ <sub>fast</sub> ms	A <sub>fast</sub> pA/pF	Fraction (%)
WT	90.7 ± 6.6 (15)	11.6 ± 1.1 <sup>a</sup>	79 ± 3 <sup>b</sup>	9.1 ± 1.7	2.9 ± 0.4	21 ± 3 <sup>b</sup>
HET	77.9 ± 7.7 (12)	6.5 ± 1.2	69 ± 4	10.1 ± 1.9	2.5 ± 0.3	31 ± 4
HOM	79.4 ± 8.9 (14)	5.9 ± 0.6	61 ± 4	7.7 ± 0.9	3.7 ± 0.4	39 ± 4

The activation phases of L-type currents evoked by test depolarizations from -50 mV to +40 mV were fitted using Eq. 4 (see Materials and methods). Data are given as mean ± SEM, with the numbers in parentheses indicating the number of myotubes tested. The analysis of activation kinetics excluded cells in which tail current decay was obviously not monoexponential.

<sup>a</sup>Significant differences among the three genotypes (P < 0.001, ANOVA).

<sup>b</sup>P < 0.005, ANOVA.

and even larger in Hom myotubes (Fig. 4 C). To quantify these differential effects, a potentiation index  $[(I_{\text{Bay K 8644}} - I_{\text{control}}) / I_{\text{control}}]$  was calculated from the average peak current at +30 mV for each genotype; the values for WT, Het, and Hom cells were 0.21, 0.39, and 0.71, respectively.

#### DHPR steady-state inactivation is shifted to hyperpolarized potentials in R163C Hom myotubes

A recent study reported that the RYR1 Y522S MHS mutation altered the voltage dependence of L-type current inactivation (Andronache et al., 2009). To determine whether the R163C mutation has a similar influence on inactivation of L-type current, we used the voltage protocol illustrated in Fig. 5 A. Specifically, 30-s prepulses to varying potentials (−50, −10, 0, 10, 20, and 30 mV) were applied before a 200-ms test depolarization to +30 mV. Importantly, an interval of >1 min at −80 mV was used between each test pulse and the subsequent prepulse to minimize the cumulative effects of holding at less negative potentials. Even with this protocol, there was an ongoing decline of the L-type current over time (unpublished data), presumably due to incomplete

removal of inactivation during the intervals at −80 mV. Thus, steady-state inactivation was measured as the fraction of the L-type current amplitude evoked by depolarization to +30 mV immediately after the 30-s prepulse divided by the L-type current amplitude evoked by a “control” depolarization to +30 mV from the −80-mV holding potential just before each prepulse. As shown in Fig. 5 B, L-type currents in WT, Het, and Hom myotubes only displayed relatively modest inactivation. Fitting of the normalized inactivation–voltage relationship for WT and Het myotubes yielded nearly equivalent half-inactivation potentials ( $V_{1/2\text{inact}} = 6.1$  and  $5.3$  mV, respectively; Fig. 5 C). The inactivation–voltage relationship for Hom myotubes ( $V_{1/2\text{inact}} = -3.3$  mV) was shifted to more hyperpolarized potentials (Fig. 5 C).

## DISCUSSION

In this study, we have used patch clamp electrophysiology to investigate effects of the MHS mutation R163C in RYR1. In particular, the function of the DHPR as voltage sensor for ECC was modified such that the dependence of SR  $\text{Ca}^{2+}$  release on membrane potential

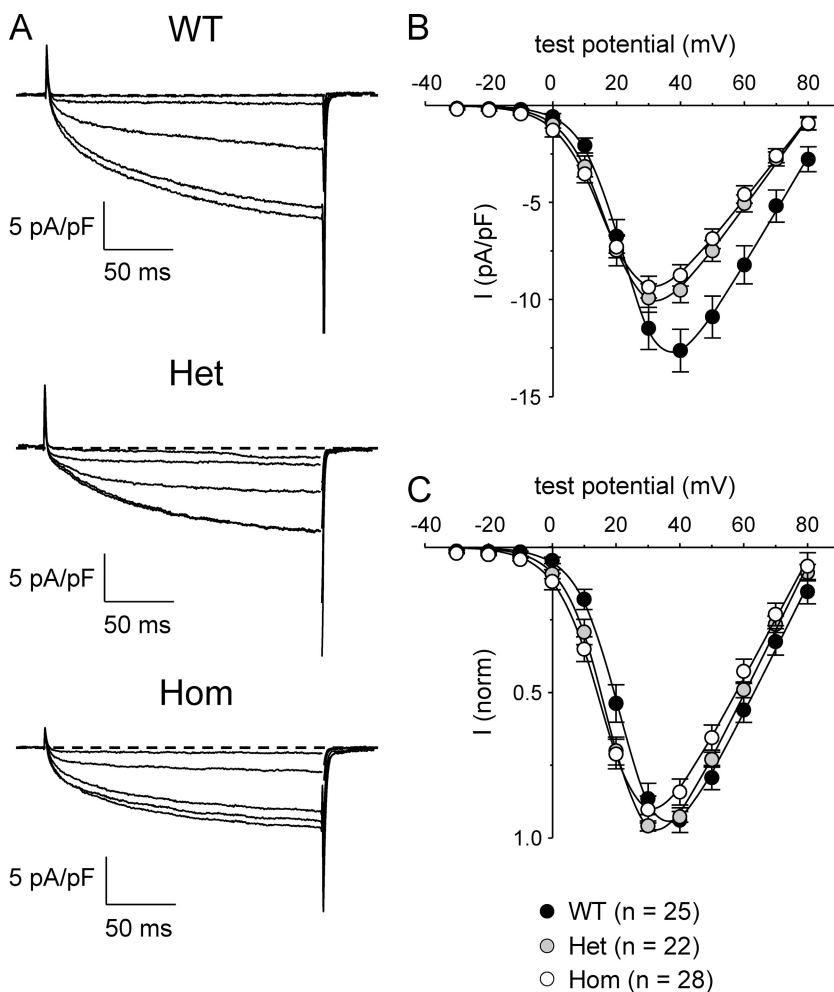


**Figure 3.** L-type currents in R163C Het and Hom myotubes are shifted to slightly more hyperpolarized potentials. (A) Representative recordings of L-type  $\text{Ca}^{2+}$  currents elicited by 200-ms depolarizations from −50 mV to test potentials of 0, 10, 20, 30, and 40 mV are shown for WT (top), Het (middle), and Hom (bottom) myotubes. (B) Comparison of peak I-V relationships for WT ( $n = 25$ ), Het ( $n = 22$ ), and Hom ( $n = 28$ ) cells. Currents were evoked at 0.1 Hz by test potentials ranging from −20 through +80 mV in 10-mV increments, following a prepulse protocol (Adams et al., 1990). Current amplitudes were normalized by linear cell capacitance (pA/pF). (C) I-V relationships for the same dataset shown in B, in which the current amplitudes have been normalized to the peak current in each cell. The smooth curves are plotted according to Eq. 3, with best-fit parameters presented in Table II.

was shifted in the hyperpolarizing direction in myotubes either Hom or Het for the R163C mutation (Fig. 1 and Table I). Hom and Het myotubes displayed hyperpolarizing shifts in the voltage dependence of the membrane-bound charge movement (Fig. 2 and Table II) that roughly paralleled the shifts in SR Ca<sup>2+</sup> release. Although smaller than the shift in charge movement, the activation of L-type currents in Hom and Het myotubes was also shifted in the hyperpolarizing direction (Fig. 3). A more striking effect of the R163C mutation on L-type channel gating was that the dihydropyridine agonist  $\pm$ Bay K 8644 caused a larger potentiation of L-type current in Het and Hom myotubes than in WT myotubes (Fig. 4). For all three genotypes, inactivation of L-type currents by 30-s prepulses occurred at relatively depolarized potentials; L-type currents in Hom myotubes inactivated at  $\sim$ 10 mV more hyperpolarized potentials than L-type current of either WT or Het myotubes (Fig. 5).

In R163C Het myotubes, there was a small hyperpolarizing shift in SR Ca<sup>2+</sup> release and a slight reduction in maximal release ( $[\Delta F/F]_{\max}$ ) relative to WT myotubes (Fig. 1 and Table I). In R163C Hom myotubes, the voltage dependence of SR Ca<sup>2+</sup> release shifted to a greater extent and maximal release was substantially reduced (Fig. 1 and Table I). As for Hom R163C myotubes, hyperpolarizing shifts in the voltage dependence of Ca<sup>2+</sup> release have also been reported for myotubes harvested from Y522S Hom mice (Chelu et al., 2006) or R615C Hom swine (Dietze et al., 2000), and for dyspedic myotubes expressing RYR1 constructs carrying several different MH mutations (Avila and Dirksen, 2001; Dirksen and Avila, 2004; Lyfenko et al., 2004). A reduction in maximal release, like that we observed in R163C Hom myotubes, was previously reported for Y522S Hom myotubes (Chelu et al., 2006). For R163C Hom myotubes, a reduced number of DHPRs (Fig. 2) is probably one contributor to the reduction in  $[\Delta F/F]_{\max}$ .

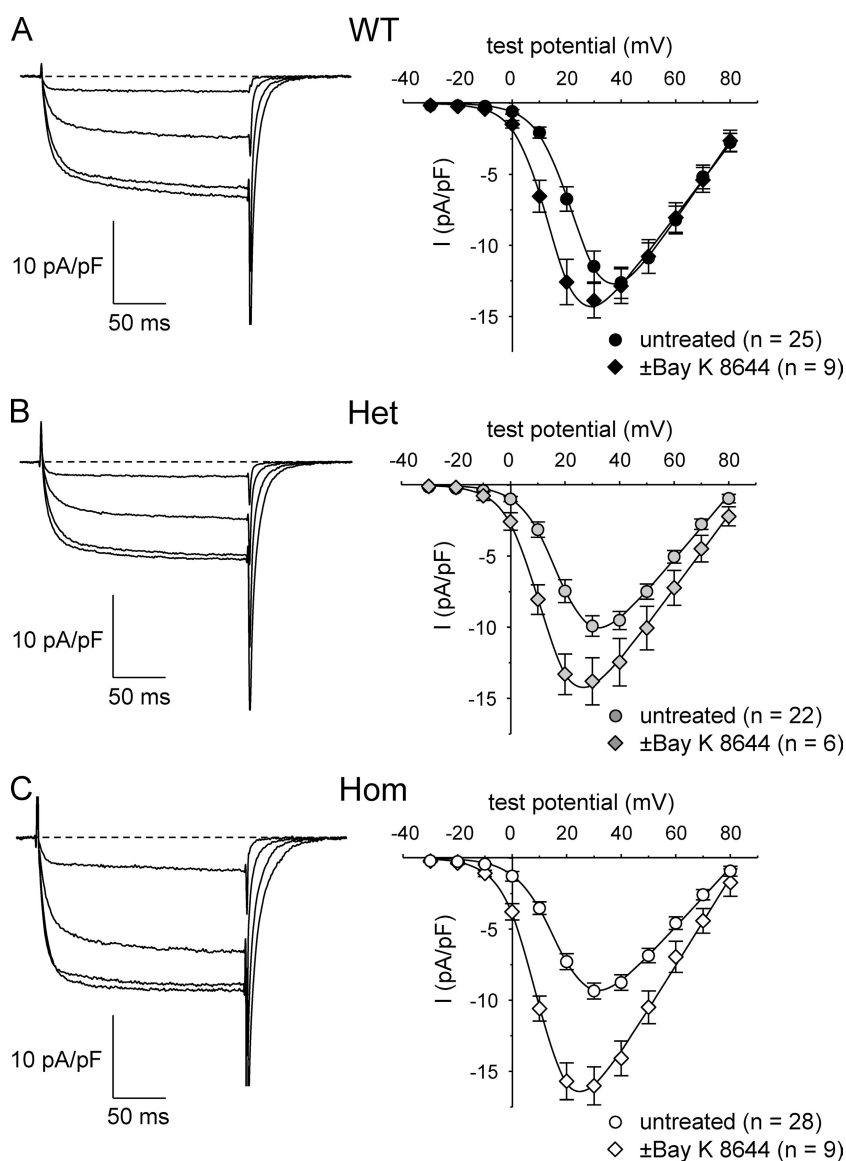


**Figure 4.** L-type currents in R163C Het and Hom myotubes are more sensitive to  $\pm$ Bay K 8644. Representative recordings of L-type currents made in the presence of  $\pm$ Bay K 8644 are shown for WT (A; left), Het (B; left), and Hom (C; left) myotubes. Currents were elicited by 200-ms depolarizations from  $-50$  mV to test potentials of 0, 10, 20, and 30 mV. The average peak I-V relationships obtained in the absence (circles) and presence (diamonds) of  $10 \mu\text{M}$   $\pm$ Bay K 8644 and are shown in A (right) for WT myotubes ( $\blacklozenge$ ,  $n = 9$ ;  $\bullet$ ,  $n = 25$ ), in B (right) for Het myotubes ( $\blacklozenge$ ,  $n = 6$ ;  $\bullet$ ,  $n = 22$ ), and in C (right) for Hom myotubes ( $\blacklozenge$ ,  $n = 9$ ;  $\circ$ ,  $n = 28$ ). Peak I-V data obtained in the absence of  $\pm$ Bay K 8644 are replotted from Fig. 3, and the smooth curves are plotted according to Eq. 3, with best-fit parameters given in Table II.

Interestingly, Lamb et al. (1989) also found a reduction in  $Q_{\max}$  ( $\sim 20\%$ ) in swine R615C Hom *gracilis* fibers. Moreover, Andronache et al. (2009) found an  $\sim 10\%$  reduction in  $Q_{\max}$  in Y522S Het *interosseus* fibers.

Corresponding to the respective  $\sim 9$ - and  $\sim 5$ -mV hyperpolarizing shifts in the voltage dependence of  $\text{Ca}^{2+}$  release for R163C Hom and Het myotubes (Table I), we also observed an  $\sim 16$ -mV hyperpolarizing shift in charge movements in Hom myotubes and a somewhat smaller shift ( $\sim 12$  mV) in Het myotubes (Fig. 2 and Table II). In an earlier study describing charge movements in swine R615C Hom fibers, Lamb et al. (1989)

did not observe a shift in charge movement. Recently, however, Andronache et al. (2009) reported a hyperpolarizing shift of  $\sim 5$  mV in charge movements of Y522S Het fibers.

Hyperpolarizing shifts in the activation of L-type current have been consistently observed in animal models of MH. In this study, we observed hyperpolarizing shifts in L-type current activation for both R163C Het and Hom ( $\sim 5$  and 7 mV, respectively). Earlier, Gallant et al. (1996) saw a small hyperpolarizing shift in R615C Hom swine myotubes but suggested that series resistance errors could have contributed to the effect. More recently,

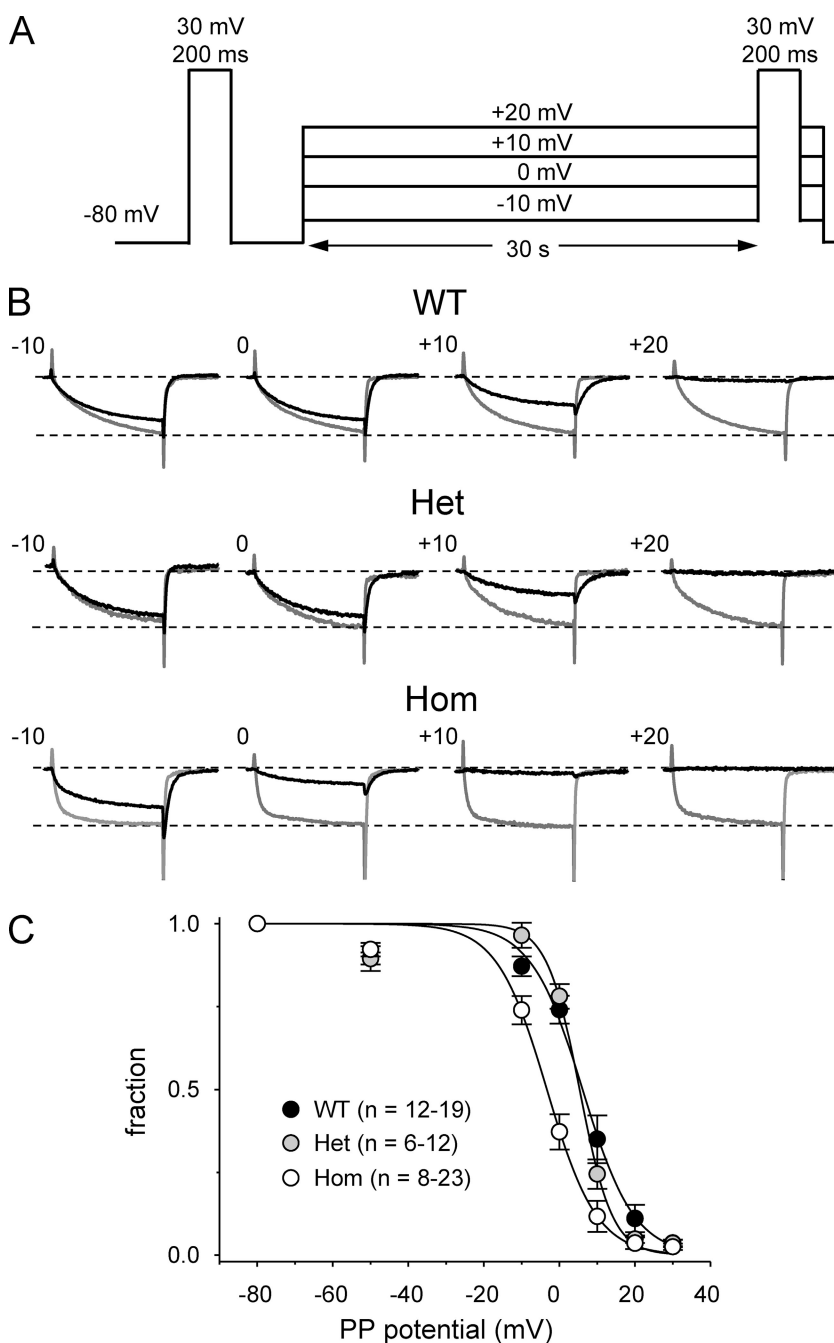


**Figure 5.** Steady-state inactivation of L-type current in WT and R163C MHS myotubes. (A) Voltage protocol. A 200-ms depolarization to +30 mV was applied just before (reference pulse) and immediately (test pulse) after 30-s prepulses to  $-50$ ,  $-10$ ,  $0$ ,  $10$ ,  $20$ , and  $30$  mV. An interval of  $>1$  min at the steady holding potential of  $-80$  mV was used between each episode of the protocol. (B) Test currents elicited with this protocol for the indicated prepulse potentials (black traces) are shown for each genotype, with the corresponding control current (gray traces) evoked before the pulse run from  $-80$  to  $+30$  mV. The amplitudes of the currents shown in B have been normalized to the amplitude of the current elicited by the reference pulse. (C) Summary of results for WT ( $n = 12-19$ ), Het ( $n = 6-12$ ), and Hom ( $n = 8-23$ ) myotubes at the indicated prepulse potentials. The average normalized inactivation values were fit by Eq. 5 (see Materials and methods), with the following respective parameters for WT, Het, and Hom myotubes:  $V_{1/2\text{inact}} = 6.1$ ,  $5.3$ , and  $-3.3$  mV;  $k = -6.8$ ,  $4.3$ , and  $6.6$  mV.

in recordings made at room temperature, hyperpolarizing shifts in the activation of L-type current have also been reported for myotubes obtained from Y522S Het ( $\sim 5$  mV; Durham et al., 2008) and Hom ( $\sim 10$  mV; see Fig. 6 B of Chelu et al., 2006) mice. A small ( $\sim 3$  mV) but significant hyperpolarizing shift in activation was observed in adult Y522S Het fibers at room temperature (Andronache et al., 2009). Although hyperpolarizing shifts in the voltage dependence of current activation were consistently observed in each of these studies, the effects of the MH mutations on the amplitude of L-type currents were variable (Fig. 3) (Lamb et al., 1989; Gallant et al., 1996; Dietze et al., 2000; Chelu et al., 2006; Durham et al., 2008; Andronache et al., 2009).

In addition to the shift in the I-V relationship for L-type currents of R163C Het and Hom myotubes, we found that this MH mutation caused an increased responsiveness to the dihydropyridine agonist  $\pm$ Bay K 8644. In particular, L-type currents of MHS R163C myotubes were potentiated to a greater degree (Hom > Het) than WT myotubes (Fig. 4). This observation suggests that one of the retrograde effects of R163C mutation on the L-type channel activity of the DHPR is to facilitate entry of the channel into the long-open gating state (i.e., mode 2; Nowycky et al., 1985), which might explain the enhanced potentiation by  $\pm$ Bay K 8644. Interestingly, Bay K 8644 enhances pharmacologically (halothane or isoflurane) induced contractures in both swine and human MHS muscle (Williams et al., 1991; Adnet et al., 1992), consistent with the idea that altered L-type current may contribute to the pathogenesis of this disease.

Compared with previous reports on the inactivation of L-type current in “normal” human myotubes (Morrill et al., 1998; Harasztosi et al., 1999), we found that the inactivation of L-type current in mouse myotubes occurred at substantially more depolarized potentials (Fig. 5). Specifically, the  $V_{1/2}$ inact for WT myotubes was  $\sim 10$ – $20$  mV more depolarized than those previously reported by Morrill et al. (1998) and Harasztosi et al. (1999). The difference between our results and those of these previous studies may reflect differences in species differences (mouse vs. human) and methodology (i.e., voltage protocol) used to assess inactivation. In adult mouse fibers, Andronache et al. (2009) reported that nearly complete inactivation ( $\sim 90\%$ ) of L-type current in WT fibers occurred after sequential prepulses (30 s each) to  $-60$ ,  $-50$ ,  $-40$ ,  $-30$ ,  $-20$ , and  $-10$  mV, and complete inactivation (100%) occurred in Y522S Het fibers. We found that L-type currents in WT and R163C Het and Hom myotubes were substantially more resistant to inactivation after 30-s prepulses, separated by 60-s epochs at  $-80$  mV. Moreover, in contrast to the findings of Andronache et al. (2009) on Y522S Het fibers, we observed little difference in inactivation between WT and R163C Het myotubes. However, an  $\sim 10$ -mV hyperpolarizing shift in inactivation was observed for R163C Hom myotubes.

Collectively, the results with whole cell voltage clamp measurements in this paper, and the results on myoplasmic  $\text{Ca}^{2+}$  transients evoked by application of elevated  $\text{K}^+$  to intact myotubes, which are described by Estève et al. in this issue, indicate that the R163C mutation in RYR1 alters the gating of the DHPR with respect both to membrane currents and ECC. Moreover, the results obtained with the two approaches are in good agreement overall. However, one difference is that peak amplitudes of  $\text{Ca}^{2+}$  transients elicited by  $\text{K}^+$  depolarization differed little between WT, R163C Het, and R163C Hom myotubes (Estève et al., 2010). In contrast,  $\text{Ca}^{2+}$  transients in response to whole cell depolarization were reduced either somewhat in R163C Het myotubes or substantially in R163C Hom myotubes (Fig. 1), which could be at least partially attributed to reduced membrane expression of the DHPR (Fig. 2). As far as why this reduced release is not seen in the measurements on intact myotubes, one possibility is a difference in  $\text{Ca}^{2+}$  buffering. Previous work (García and Beam, 1994) has shown that  $\text{Ca}^{2+}$ -induced  $\text{Ca}^{2+}$  release contributes to depolarization-evoked  $\text{Ca}^{2+}$  transients in myotubes when the pipette solution has weak  $\text{Ca}^{2+}$  buffering (0.1 mM EGTA), but not when it has stronger buffering. Thus, intact R163C Het or Hom myotubes may have enhanced  $\text{Ca}^{2+}$ -induced  $\text{Ca}^{2+}$  release, which can compensate for a reduction in SR  $\text{Ca}^{2+}$  release that is directly voltage gated.

At least superficially, there also appears to be a discrepancy between the whole cell measurements of L-type  $\text{Ca}^{2+}$  current and the small enhancement in extracellular  $\text{Ca}^{2+}$  entry in R163C Het and Hom myotubes inferred from  $\text{Ca}^{2+}$  transients in response to  $\text{K}^+$  depolarization (Fig. 5 of Estève et al., 2010) because there was actually a small reduction in the maximal amplitude of whole cell  $\text{Ca}^{2+}$  currents in Het and Hom myotubes (Fig. 3). However, it is important to note that the hyperpolarizing shifts in the activation of L-type current in R163C Het and Hom myotubes ( $\sim 5$  and  $\sim 7$  mV, respectively; Table II) mean that the currents in response to weak depolarizations were actually larger in the mutant myotubes than in WT (Fig. 3 B). These small hyperpolarizing shifts would likely be of particular importance for the response of intact myotubes to 60 mM  $\text{K}^+$ , which was shown to produce depolarizations to about  $-13$  mV (Table I of Estève et al., 2010), a level that is just barely above threshold for eliciting inward  $\text{Ca}^{2+}$  current in myotubes bathed in 2 mM  $\text{Ca}^{2+}$  (Fig. 4 of Bannister et al., 2009b). A hyperpolarizing shift in activation of skeletal L-type channels, which have been shown to be permeant to  $\text{Mn}^{2+}$  (Bannister et al., 2009b), may also explain the increased  $\text{Mn}^{2+}$  entry observed in R163C Het and Hom myotubes in response to  $\text{K}^+$  depolarization (Fig. 6 of Estève et al., 2010).

Importantly, both the whole cell voltage clamp and  $\text{K}^+$  depolarization experiments demonstrated that the R163C mutation causes a hyperpolarizing shift in  $\text{Ca}^{2+}$  release,

which was shown by the whole cell measurements to be accompanied by a similar shift in voltage sensor charge movements. Fig. 6 presents a qualitative model that can account for this shift and some of the other effects of the R163C mutation on DHPR gating. The model is based on the simple idea that the free energy for activation of RYR1 upon depolarization, and its deactivation upon repolarization, is provided by the movement of DHPR charged residues (designated “Q” in Fig. 6) through the membrane field. If this idea is correct, then just as the transition of the DHPR from resting to ECC activated would promote the corresponding transition of RYR1, alterations of RYR1 that promoted its entry into the ECC-activated conformation would facilitate the corresponding transition of the DHPR. The R163C mutation has been shown to cause RYR1 to be activated more easily by agonists (Yang et al., 2006), which may indicate that it enters more easily into the ECC-activated conformation. If this is the case, it may explain the hyperpolarizing shift in the Q-V relationship in R163C Het and Hom myotubes (Fig. 2). It also seems reasonable that although there is a hyperpolarizing shift in the activation of L-type current in R163C Het and Hom myotubes (Fig. 3), this shift is less than that for the Q-V relationship because the activation of the L-type current depends not only on the movement of Q, but also on that of an additional charge (“q” in Fig. 6). This additional charge is smaller than Q, moves more slowly, and moves at potentials that are rightward shifted relative to those that cause RYR1 to enter the ECC-activated state (Dirksen and Beam, 1999). Accordingly, the R163C mutation would not have a direct effect on the movement of q, and the hyperpolarizing shift in L-type channel activation would be a “mass-action” consequence of the hyperpolarizing shift in the movement of Q and the resulting loading of the state of the DHPR just before L-type channel opening. If the inactivation of L-type current proceeds primarily from the open state of the channel, the hyperpolarizing shift in the activation of current would be accompanied by a hyperpolarizing shift in the voltage dependence of inactivation (Fig. 5 C).

One of the major features observed in the K<sup>+</sup> depolarization experiments is that the inactivation of ECC during prolonged depolarization was slowed in R163C Het and Hom myotubes (Figs. 1 and 7 of Estève et al., 2010). Because the inactivation of ECC leads to a cessation of SR Ca<sup>2+</sup> release via RYR1, it seems reasonable to hypothesize that cytoplasmic domains of the DHPR, and the foot of RYR1, assume a different conformation than in the ECC-activated state (Fig. 6). If, as hypothesized above, the R163C mutation stabilizes the ECC-activated state of the RYR1 foot domain, it would be expected to slow the rate of entry of the DHPR and RYR1 into the ECC-inactivated state.

In conclusion, our work now shows that voltage-driven transitions of the skeletal muscle DHPR are affected by mutations that alter the function, and presumably the

conformation, of RYR1. Collectively, our present results and those presented in the companion paper (Estève et al., 2010) support the idea that the altered retrograde conformational coupling can affect the function

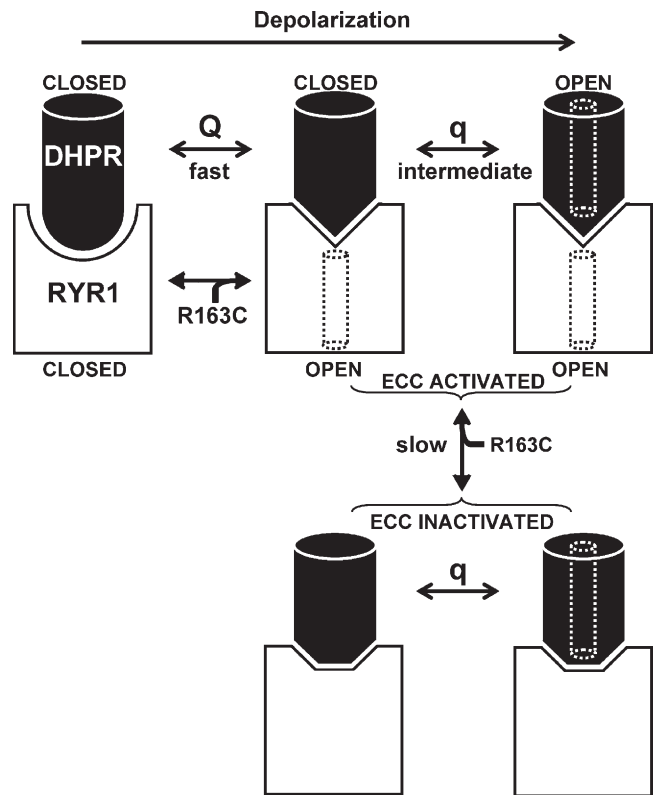


**Figure 6.** A model that can account for the effects on DHPR gating, which result from the R163C mutation in RYR1. In the model, the major component of DHPR gating charge (Q) moves rapidly (milliseconds) upon depolarization and results in a conformational change of a DHPR cytoplasmic domain(s) from “resting” to “ECC activating,” which in turn triggers a corresponding conformational change in the cytoplasmic (“foot”) domain of RYR1 that opens the RYR1 pore (black dotted cylinder). Although the movement of Q is necessary for the activation of L-type current via the DHPR, it is not sufficient. Opening of the L-type channel pore (white dotted cylinder) additionally depends on another DHPR charge (q), which moves more slowly (tens of milliseconds), is smaller than Q, and moves at more depolarized potentials than those causing ECC Ca<sup>2+</sup> release (Dirksen and Beam, 1999). The R163C MHS mutation shifts the equilibrium of RYR1 toward the open state (Yang et al., 2003, 2006), and if this open state is linked to the ECC-activated conformation of the foot domain, it would retrogradely promote the ECC-activating conformation of the DHPR, with the result that less depolarization would be required to move Q (Fig. 2). The hyperpolarizing shift in the movement of Q also causes a hyperpolarizing shift in activation of the L-type channel (Fig. 3), but this shift is less pronounced because the movement of q is not directly affected by the transition of RYR1 to the ECC-activated state. During prolonged depolarization (tens of seconds), the DHPR shifts to a state that is inactivated for ECC (Beam and Horowicz, 2004). Entry into this ECC-inactivated state is slowed (Figs. 1 and 7 of Estève et al., 2010) because the ECC-activated states of RYR1 (and thus the DHPR) are stabilized by the R163C MHS mutation.

of the DHPR as both ECC voltage sensor and as L-type  $\text{Ca}^{2+}$  channel.

We thank Dr. J.D. Ohrtman and Ms. Ong Moua for insightful discussion.

This work was supported by grants from the Muscular Dystrophy Association (MDA4155 to R.A. Bannister and MDA4319 to K.G. Beam), the Foundation Recherche Medical (SPE20040901554 to E. Estève), and the National Institutes of Health (NIH P01AR052534 to P.D. Allen and I.N. Pessah, and AR44750 to K.G. Beam).

Kenneth C. Holmes served as editor.

Submitted: 18 September 2009

Accepted: 20 April 2010

## REFERENCES

- Adams, B.A., and K.G. Beam. 1989. A novel calcium current in dysgenic skeletal muscle. *J. Gen. Physiol.* 94:429–444. doi:10.1085/jgp.94.3.429
- Adams, B.A., T. Tanabe, A. Mikami, S. Numa, and K.G. Beam. 1990. Intramembrane charge movement restored in dysgenic skeletal muscle by injection of dihydropyridine receptor cDNAs. *Nature.* 346:569–572. doi:10.1038/346569a0
- Adnet, P.J., R.M. Krivosic-Horber, M.M. Adamantidis, G. Haudecoeur, H. Reyford, and M. Imbenotte. 1992. Effect of Bay K 8644 on the magnitude of isoflurane and halothane contracture of skeletal muscle from patients susceptible to malignant hyperthermia. *Anesthesiology.* 76:544–549. doi:10.1097/0000542-199204000-00010
- Ahern, C.A., D.C. Sheridan, W. Cheng, L. Mortenson, P. Nataraj, P.D. Allen, M. De Waard, and R. Coronado. 2003.  $\text{Ca}^{2+}$  current and charge movements in skeletal myotubes promoted by the  $\beta$ -subunit of the dihydropyridine receptor in the absence of ryanodine receptor type 1. *Biophys. J.* 84:942–959. doi:10.1016/S0006-3495(03)74911-X
- Andronache, Z., S.L. Hamilton, R.T. Dirksen, and W. Melzer. 2009. A retrograde signal from RyR1 alters DHP receptor inactivation and limits window  $\text{Ca}^{2+}$  release in muscle fibers of Y522S RyR1 knock-in mice. *Proc. Natl. Acad. Sci. USA.* 106:4531–4536. doi:10.1073/pnas.0812661106
- Armstrong, C.M., F.M. Bezanilla, and P. Horowicz. 1972. Twitches in the presence of ethylene glycol bis-(aminoethyl ether)-N,N'-tetracetic acid. *Biochim. Biophys. Acta.* 267:605–608. doi:10.1016/0005-2728(72)90194-6
- Avila, G., and R.T. Dirksen. 2000. Functional impact of the ryanodine receptor on the skeletal muscle L-type  $\text{Ca}^{2+}$  channel. *J. Gen. Physiol.* 115:467–480. doi:10.1085/jgp.115.4.467
- Avila, G., and R.T. Dirksen. 2001. Functional effects of central core disease mutations in the cytoplasmic region of the skeletal muscle ryanodine receptor. *J. Gen. Physiol.* 118:277–290. doi:10.1085/jgp.118.3.277
- Bannister, R.A., and K.G. Beam. 2009. Ryanodine modification of RyR1 retrogradely affects L-type  $\text{Ca}^{2+}$  channel gating in skeletal muscle. *J. Muscle Res. Cell Motil.* 30:217–223. doi:10.1007/s10974-009-9190-0
- Bannister, R.A., H.M. Colecraft, and K.G. Beam. 2008a. Rem inhibits skeletal muscle EC coupling by reducing the number of functional L-type  $\text{Ca}^{2+}$  channels. *Biophys. J.* 94:2631–2638. doi:10.1529/biophysj.107.116467
- Bannister, R.A., M. Grabner, and K.G. Beam. 2008b. The  $\alpha_{1S}$  III-IV loop influences 1,4-dihydropyridine receptor gating but is not directly involved in excitation-contraction coupling interactions with the type I ryanodine receptor. *J. Biol. Chem.* 283:23217–23223. doi:10.1074/jbc.M804312200
- Bannister, R.A., S. Papadopoulos, C.S. Haarmann, and K.G. Beam. 2009a. Effects of inserting fluorescent proteins into the  $\alpha_{1S}$  II–III loop: insights into excitation–contraction coupling. *J. Gen. Physiol.* 134:35–51. doi:10.1085/jgp.200910241
- Bannister, R.A., I.N. Pessah, and K.G. Beam. 2009b. The skeletal L-type  $\text{Ca}^{2+}$  current is a major contributor to excitation-coupled  $\text{Ca}^{2+}$  entry. *J. Gen. Physiol.* 133:79–91. doi:10.1085/jgp.200810105
- Beam, K.G., and P. Horowicz. 2004. Excitation-contraction coupling in skeletal muscle. In *Myology*, A.G. Engel and C. Franzini-Armstrong, editors. McGraw-Hill, New York. 257–280.
- Beam, K.G., and C.M. Knudson. 1988. Calcium currents in embryonic and neonatal mammalian skeletal muscle. *J. Gen. Physiol.* 91:781–798. doi:10.1085/jgp.91.6.781
- Block, B.A., T. Imagawa, K.P. Campbell, and C. Franzini-Armstrong. 1988. Structural evidence for direct interaction of the molecular components of the transverse tubule/sarcoplasmic reticulum junction in skeletal muscle. *J. Cell Biol.* 107:2587–2600. doi:10.1083/jcb.107.6.2587
- Chelu, M.G., S.A. Goonasekera, W.J. Durham, W. Tang, J.D. Lueck, J. Riehl, I.N. Pessah, P. Zhang, M.B. Bhattacharjee, R.T. Dirksen, and S.L. Hamilton. 2006. Heat- and anesthesia-induced malignant hyperthermia in an RyR1 knock-in mouse. *FASEB J.* 20:329–330.
- Cherednichenko, G., C.W. Ward, W. Feng, E. Cabrales, L. Michaelson, M. Sámso, J.R. López, P.D. Allen, and I.N. Pessah. 2008. Enhanced excitation-coupled calcium entry in myotubes expressing malignant hyperthermia mutation R163C is attenuated by dantrolene. *Mol. Pharmacol.* 73:1203–1212. doi:10.1124/mol.107.043299
- Dietze, B., J. Henke, H.M. Eichinger, F. Lehmann-Horn, and W. Melzer. 2000. Malignant hyperthermia mutation Arg615Cys in the porcine ryanodine receptor alters voltage dependence of  $\text{Ca}^{2+}$  release. *J. Physiol.* 526:507–514. doi:10.1111/j.1469-7793.2000.t01-1-00507.x
- Dirksen, R.T., and G. Avila. 2004. Distinct effects on  $\text{Ca}^{2+}$  handling caused by malignant hyperthermia and central core disease mutations in RyR1. *Biophys. J.* 87:3193–3204. doi:10.1529/biophysj.104.048447
- Dirksen, R.T., and K.G. Beam. 1999. Role of calcium permeation in dihydropyridine receptor function. Insights into channel gating and excitation-contraction coupling. *J. Gen. Physiol.* 114:393–403. doi:10.1085/jgp.114.3.393
- Durham, W.J., P. Aracena-Parks, C. Long, A.E. Rossi, S.A. Goonasekera, S. Boncompagni, D.L. Galvan, C.P. Gilman, M.R. Baker, N. Shirokova, et al. 2008. RyR1 S-nitrosylation underlies environmental heat stroke and sudden death in Y522S RyR1 knockin mice. *Cell.* 133:53–65. doi:10.1016/j.cell.2008.02.042
- Estève, E., K. Liu, J.M. Eltit, R.A. Bannister, K.G. Beam, P.D. Allen, I.N. Pessah, and J. López. 2010. A malignant hyperthermia-inducing mutation in RYR1 (R163C): alterations in  $\text{Ca}^{2+}$  entry, release, and retrograde signaling to the DHPR. *J. Gen. Physiol.* 135:619–628.
- Gallant, E.M., E.M. Balog, and K.G. Beam. 1996. Slow calcium current is not reduced in malignant hyperthermic porcine myotubes. *Muscle Nerve.* 19:450–455. doi:10.1002/(SICI)1097-4598(199604)19:4<450::AID-MUS4>3.0.CO;2-B
- García, J., and K.G. Beam. 1994. Measurement of calcium transients and slow calcium current in myotubes. *J. Gen. Physiol.* 103:107–123. doi:10.1085/jgp.103.1.107
- Grabner, M., R.T. Dirksen, N. Suda, and K.G. Beam. 1999. The II–III loop of the skeletal muscle dihydropyridine receptor is responsible for the bi-directional coupling with the ryanodine receptor. *J. Biol. Chem.* 274:21913–21919. doi:10.1074/jbc.274.31.21913
- Harasztosi, C., I. Sipos, L. Kovács, and W. Melzer. 1999. Kinetics of inactivation and restoration from inactivation of the L-type calcium current in human myotubes. *J. Physiol.* 516:129–138. doi:10.1111/j.1469-7793.1999.129aa.x

- Hurne, A.M., J.J. O'Brien, D. Wingrove, G. Cherednichenko, P.D. Allen, K.G. Beam, and I.N. Pessah. 2005. Ryanodine receptor type 1 (RyR1) mutations C4958S and C4961S reveal excitation-coupled calcium entry (ECCE) is independent of sarcoplasmic reticulum store depletion. *J. Biol. Chem.* 280:36994–37004. doi:10.1074/jbc.M506441200
- Lamb, G.D., K.C. Hopkinson, and M.A. Denborough. 1989. Calcium currents and asymmetric charge movement in malignant hyperpyrexia. *Muscle Nerve.* 12:135–140. doi:10.1002/mus.880120208
- Lyfenko, A.D., S.A. Goonasekera, and R.T. Dirksen. 2004. Dynamic alterations in myoplasmic Ca<sup>2+</sup> in malignant hyperthermia and central core disease. *Biochem. Biophys. Res. Commun.* 322:1256–1266. doi:10.1016/j.bbrc.2004.08.031
- Morrill, J.A., R.H. Brown Jr., and S.C. Cannon. 1998. Gating of the L-type Ca channel in human skeletal myotubes: an activation defect caused by the hypokalemic periodic paralysis mutation R528H. *J. Neurosci.* 18:10320–10334.
- Nakai, J., R.T. Dirksen, H.T. Nguyen, I.N. Pessah, K.G. Beam, and P.D. Allen. 1996. Enhanced dihydropyridine receptor channel activity in the presence of ryanodine receptor. *Nature.* 380:72–75. doi:10.1038/380072a0
- Nowycky, M.C., A.P. Fox, and R.W. Tsien. 1985. Long-opening mode of gating of neuronal calcium channels and its promotion by the dihydropyridine calcium agonist Bay K 8644. *Proc. Natl. Acad. Sci. USA.* 82:2178–2182. doi:10.1073/pnas.82.7.2178
- Paolini, C., J.D. Fessenden, I.N. Pessah, and C. Franzini-Armstrong. 2004. Evidence for conformational coupling between two calcium channels. *Proc. Natl. Acad. Sci. USA.* 101:12748–12752. doi:10.1073/pnas.0404836101
- Protasi, F., C. Paolini, J. Nakai, K.G. Beam, C. Franzini-Armstrong, and P.D. Allen. 2002. Multiple regions of RyR1 mediate functional and structural interactions with  $\alpha_{(1\delta)}$ -dihydropyridine receptors in skeletal muscle. *Biophys. J.* 83:3230–3244. doi:10.1016/S0006-3495(02)75325-3
- Rando, T.A., and H.M. Blau. 1994. Primary mouse myoblast purification, characterization, and transplantation for cell-mediated gene therapy. *J. Cell Biol.* 125:1275–1287. doi:10.1083/jcb.125.6.1275
- Ríos, E., and G. Brum. 1987. Involvement of dihydropyridine receptors in excitation-contraction coupling in skeletal muscle. *Nature.* 325:717–720. doi:10.1038/325717a0
- Schneider, M.F., and W.K. Chandler. 1973. Voltage dependent charge movement of skeletal muscle: a possible step in excitation-contraction coupling. *Nature.* 242:244–246. doi:10.1038/242244a0
- Sheridan, D.C., H. Takekura, C. Franzini-Armstrong, K.G. Beam, P.D. Allen, and C.F. Perez. 2006. Bidirectional signaling between calcium channels of skeletal muscle requires multiple direct and indirect interactions. *Proc. Natl. Acad. Sci. USA.* 103:19760–19765. doi:10.1073/pnas.0609473103
- Takekura, H., L. Bennett, T. Tanabe, K.G. Beam, and C. Franzini-Armstrong. 1994. Restoration of junctional tetrads in dysgenic myotubes by dihydropyridine receptor cDNA. *Biophys. J.* 67:793–803. doi:10.1016/S0006-3495(94)80539-9
- Takekura, H., C. Paolini, C. Franzini-Armstrong, G. Kugler, M. Grabner, and B.E. Flucher. 2004. Differential contribution of skeletal and cardiac II-III loop sequences to the assembly of dihydropyridine-receptor arrays in skeletal muscle. *Mol. Biol. Cell.* 15:5408–5419. doi:10.1091/mbc.E04-05-0414
- Tanabe, T., K.G. Beam, J.A. Powell, and S. Numa. 1988. Restoration of excitation-contraction coupling and slow calcium current in dysgenic muscle by dihydropyridine receptor complementary DNA. *Nature.* 336:134–139. doi:10.1038/336134a0
- Tanabe, T., K.G. Beam, B.A. Adams, T. Niidome, and S. Numa. 1990. Regions of the skeletal muscle dihydropyridine receptor critical for excitation-contraction coupling. *Nature.* 346:567–569. doi:10.1038/346567a0
- Williams, J.H., M. Holland, J.C. Lee, C.W. Ward, and C.J. McGrath. 1991. BAY K 8644 and nifedipine alter halothane but not caffeine contractures of malignant hyperthermic muscle fibers. *Am. J. Physiol.* 261:R782–R786.
- Yang, T., T.A. Ta, I.N. Pessah, and P.D. Allen. 2003. Functional defects in six ryanodine receptor isoform-I (RyR1) mutations associated with malignant hyperthermia and their impact on skeletal excitation-contraction coupling. *J. Biol. Chem.* 278:25722–25730. doi:10.1074/jbc.M302165200
- Yang, T., J. Riehl, E. Estève, K.I. Matthaehi, S. Goth, P.D. Allen, I.N. Pessah, and J.R. López. 2006. Pharmacologic and functional characterization of malignant hyperthermia in the R163C RyR1 knock-in mouse. *Anesthesiology.* 105:1164–1175. doi:10.1097/00000542-200612000-00016